ELSEVIER

Journal of Alloys and Compounds 321 (2001) 248–260

Journal of ALLOYS AND COMPOUNDS

www.elsevier.com/locate/jallcom

Comments on the formation thermodynamics of selected groups of rare earth compounds

Riccardo Ferro*, Gabriella Borzone, Nadia Parodi

Dipartimento di Chimica e Chimica Industriale, Sezione di Chimica Inorganica e Metallurgia, Via Dodecaneso 31, Università di Genova, I-16146 Genova, Italy

Received 5 September 2000; accepted 5 December 2000

Abstract

In the framework of a description of the general alloying behaviour of the rare earth (R) metals, their reaction thermochemistry is reviewed. Problems met in the thermochemical characterization and in the experimental investigation of R alloys and compounds are highlighted and discussed. A short summary of the work in this field, carried out in our laboratory is reported. Special attention is given to the work performed and in progress on selected groups of R compounds: these are aurides, arsenides, antimonides, bismuthides and tellurides. The results obtained in the standard enthalpy measurements by direct calorimetry for RAu compounds, La–As, Tb–Bi and Ce–Te solid alloys are reported and discussed. Typical values of $\Delta_f H^0$ (kJ/mol at. at 300 K) are: LaAu, -72.0 ± 2.0; Ce_2Au, -55.0 ± 1.0; GdAu, -82.0 ± 2.0; TbAu, -82.0 ± 2.0; DyAu, -82.0 ± 3.0; HoAu, -83.0 ± 4.0; YbAu, -75.0 ± 2.0, LaAs, -150.0 ± 3.0, TbBi, -104.0 ± 2.0; CeTe, -168 ± 4 and Ce_3Te_4–Ce_2Te_3, -163 ± 4.

Keywords: Thermochemistry; Formation enthalpy; Rare earth alloys; Rare earth aurides; Rare earth pnictides; Rare earth chalcogenides

1. Introduction and general remarks on rare earth alloy thermochemistry

In this contribution a short summary will be given on some topics concerning the thermochemistry of the rare earth (R) alloys, presenting some details about the work we have now in progress. Special attention will be given to a few groups of alloys characterized by high values of the formation enthalpies. In order to set this point, we may refer to Fig. 1 which is an overall summary of the thermochemical behaviour of the rare earth metals: an indication is indeed given on the formation enthalpies of the different R–Me alloys as a function of the position of Me in the Periodic Table. This behaviour changes, but slightly, from one rare earth to another, and this is an interesting point worthwhile discussing later (especially considering the different subdivision of the series of rare earths into 'light' and 'heavy', trivalent and divalent, etc.).

On the basis of Fig. 1, however, it is possible to discuss in a first approximation, an average trend. For the different elements an indication is given of the maximum negative values observed at room temperature for the ΔH of formation of solid alloys in their binary systems with the 'trivalent' R. The ΔH minima in some cases (for instance with the elements such as Au, As, Sb, Bi, Te, etc.) correspond to the equiatomic composition; in several cases, however, other stoichiometries (for instance 1:2 in the R–Al alloys) correspond to the most stable solid phases.

The trend, presented in Fig. 1, of the formation enthalpies, may be related to the stability of the intermediate phases and, more generally, to the compound formation capability shown by an 'average' R with the different elements.

It is known, indeed, that, from this point of view, a characteristic subdivision of the different elements into two sets may be considered. Generally, the elements placed on the left (in the first groups, with the exception of H, Be and Mg) in the Periodic Table do not form intermediate compounds with the R. Their phase diagrams are of the simple eutectic or monotectic types, and we have here either zero or very small (negative or positive) values of ΔH of formation.

With the elements on the right of the Periodic Table, on the other hand, we have clearly negative values of the $\Delta_f H$ and the formation of a certain number of intermediate

*Corresponding author. Tel.: +39-010-353-6149; fax: +39-010-362-5051.

E-mail address: ferro@chimica.unige.it (R. Ferro).

0925-8388/01/$ – see front matter
PII: S0925-8388(01)00969-0

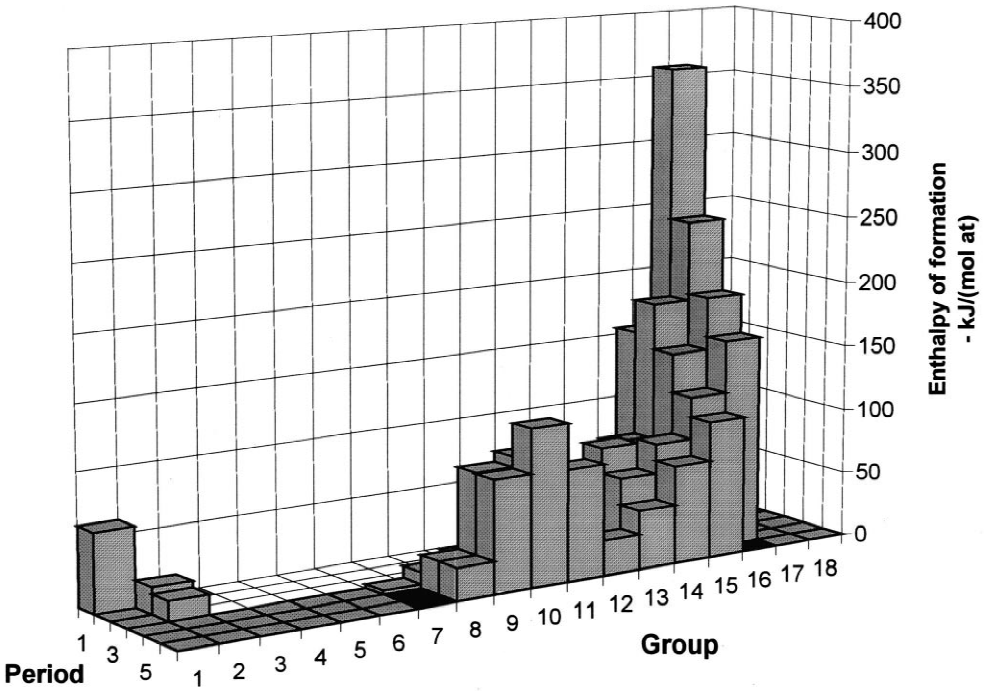

Fig. 1. Formation enthalpies (averaged values) of the trivalent rare earth solid alloys with the different elements in the Periodic Table. Generally, the more negative value observed in the R–Me systems with a given Me is reported (compare with Fig. 15). Black cells correspond to the elements for which no reliable data are available. The halogenides have not been considered.

phases. This trend may be shown in greater detail by considering the change in the shape of the phase diagrams (and in the corresponding melting points) formed together with the R by the different elements along a row of the Periodic Table. The 6th row is here presented as an example in Fig. 2, where the available known diagrams given by Gd (in a few cases by Y) have been selected [1].

Considering now the elements which form compounds with the R metals (that is the elements from the 7th to the 17th group) we may notice two families of very stable compounds: those given with 'noble metals' and those (having an increasing covalent/ionic character) formed with the metals, semi-metals and finally non-metals at the far right end of the Periodic Table.

The contribution given by Ole Kleppa and co-workers to the systematics of the R thermochemistry is well known. A high number of alloys have been studied by them and their accurate, elegant measurements, for instance on the compounds with the noble metals [2,3] are very important.

As for our group in Genova, for some time now we have been involved in the investigation of some groups of rare earth alloys generally having clearly exothermal characteristics, among which those with the elements of the 14th, 15th, 16th groups and also, for instance, with Ni and Au.

2. Experimental direct reaction calorimetry

As previously mentioned, we have generally studied alloys having high negative values of the ΔH of formation and we have used calorimeters built in our laboratory. These have been designed considering the peculiar characteristics of the R metal and alloys (mainly their high general reactivity, oxidability, etc.) and are based on the 'direct' methods.

2.1. Direct reaction calorimetry

According to this technique, the reaction, i.e. the synthesis of the alloy, takes place in the calorimeter itself.

Several examples of techniques have been presented according to which intermetallic compounds are synthesized inside the calorimeter from a convenient mixture of the component metals. A special case is that of the 'self-propagating reactions' (gas-free combustion synthesis). Many mixtures of solid substances (capable of reacting with a strong thermal evolution) if heated up to a certain characteristic temperature, may give rise to a self-sustained reaction leading to the combination of the initial substances.

Different kinds of calorimeters have been employed for measuring the heat evolved by these reactions. A point common to all these techniques is the necessity of starting the reaction inside the mixture and having it running in a controlled manner. Different ignition methods have been suggested and used; reference can be made to them for a classification of these calorimeters.

In any case, state and composition of the sample have to be checked (preferably, when possible, before and after the thermal measurements) that is, the elemental as well as the

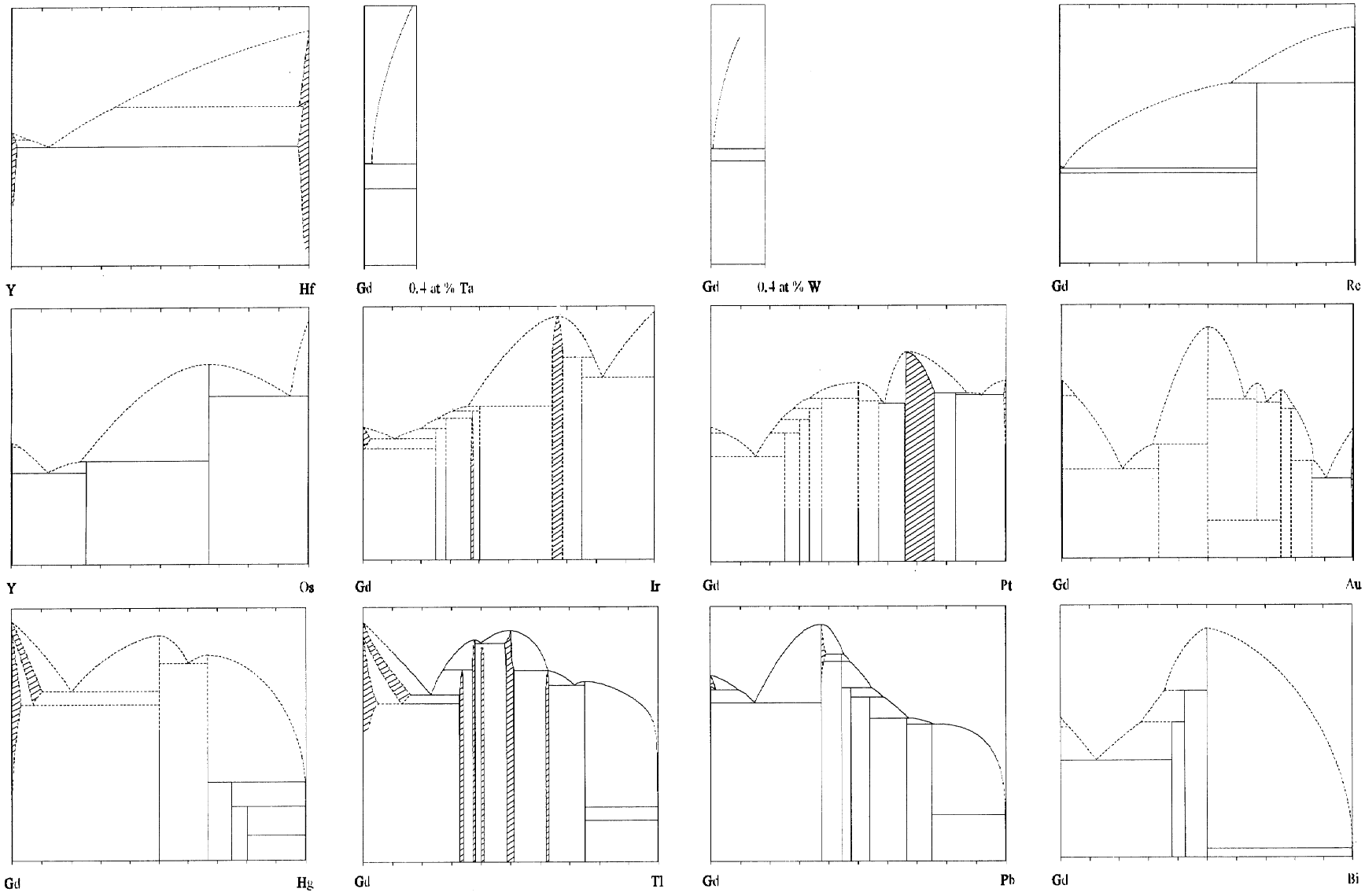

Fig. 2. R–Me phase diagrams (at%) of trivalent rare earths (Gd, in two cases Y) with the elements of the 6th row of the Periodic Table [1]. Note the changes of the temperature scale (and, in two cases, composition scale) from one diagram to another, according to the melting temperature of the Me partners. Notice several uncertainties (mainly in the liquidus) in the shape of the phase diagrams (dotted lines).

phase composition have to be clearly defined. To this end, microscopy, microprobe and X-ray diffraction analyses, have generally been used.

Two types of direct calorimeters have been built in our laboratory for the measurements of the formation enthalpies: a room-temperature and a high-temperature calorimeter.

2.1.1. Room-temperature direct synthesis calorimetry

This type of instrument is enclosed inside a room temperature water-thermostat and, even though at the start of the reaction there is self-heating of the sample, during the measurement the temperature of the calorimeter (and of the sample inside it, etc.) cools down again to room temperature. A popular calorimeter of this group is the so-called *small-furnace calorimeter* (Öfchen-Kalorimeter) [4]. In principle a mixture of the powders of the two component metals is heated by a small furnace within a calorimeter until alloying takes place. The electrical energy supplied is measured and subtracted from the total heat evolved. The electric energy dissipated in the calorimeter in the reaction run is then compared with that needed to obtain the same temperature/time response in a number of calibration runs. Our instrument, as sketched in Fig. 3, is based on these characteristics [5,6]; it consists of an aluminium cylinder which contains two small electric

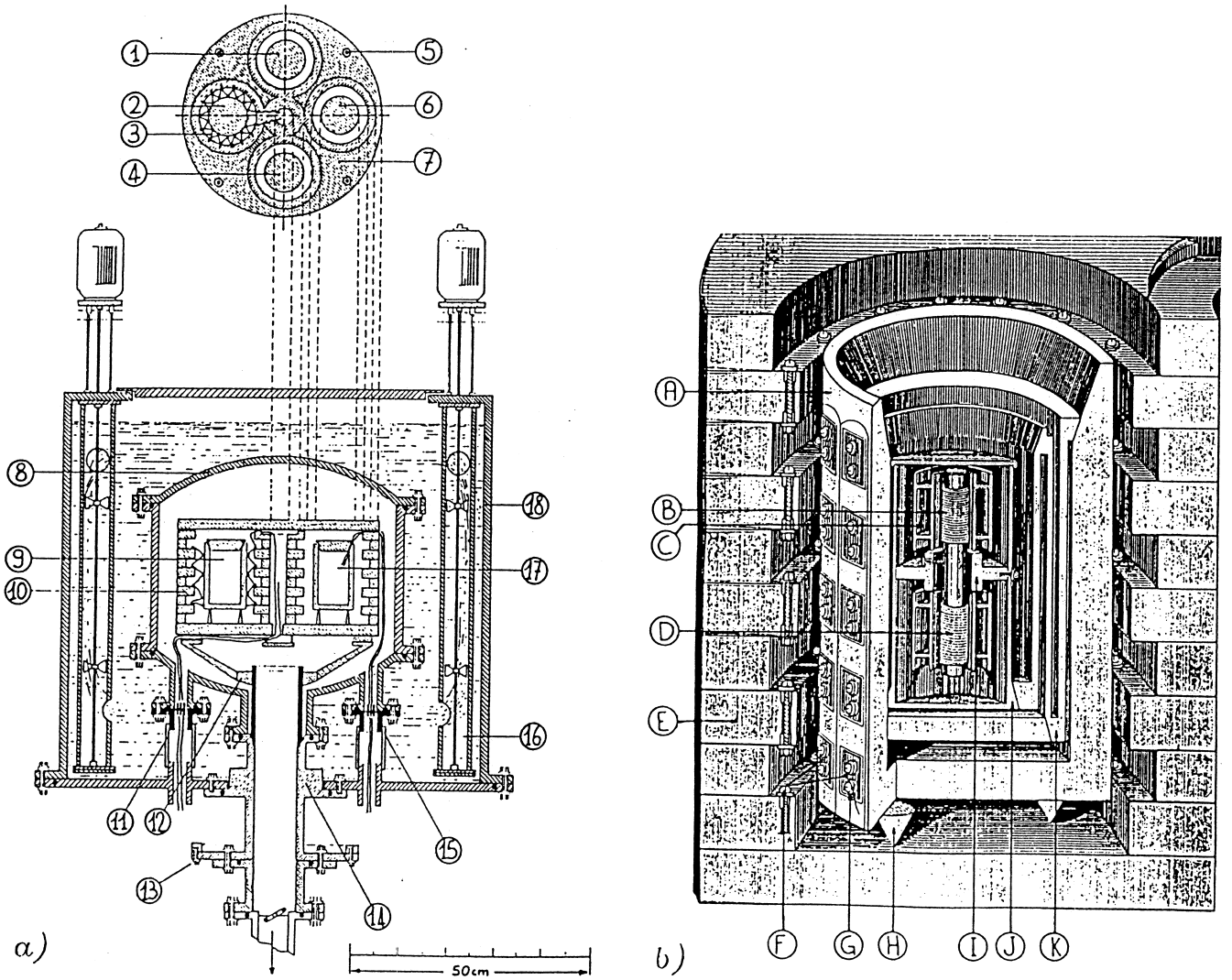

Fig. 3. Aneroid small-furnace calorimeter. (Reprinted from [6] by courtesy of ASM International®, The Materials Information Society). (a) In the upper part the horizontal section of the thermostatic block (7) is shown. It consists of aluminium discs placed one on top of the other and rigidly connected by the bolts (5), in which four identical calorimeters (1), (2), (4) and (6) are symmetrically arranged. A thermopile (3) is schematically presented. In the vertical section two opposite calorimeters (9) and (17) ((2) and (6) in the horizontal section) placed in the thermostatic block (10, 7) are shown. Their thermopiles are differentially connected. The envelope (8) is contained in an ultrathermostat (18) with propellers (16) and has a central hole for argon/vacuum connection. (11) and (15) are the feed for the electric and thermopile wires, (12), (13) and (14) are supports of the different parts of the equipment. (b) View of one calorimeter. (A) is the external part of the calorimeter and (C) is a double cylinder container of the sample surrounding the heaters. (B) and (D) are the heaters of the sample and for calibration of an inert metallic block similar to the sample. (F) and (G) are thermopile junctions and (E) is the reference block. (J) and (K) are thermal resistance connecting the platform (I) to the external surface of the calorimeter. (H) is a support.

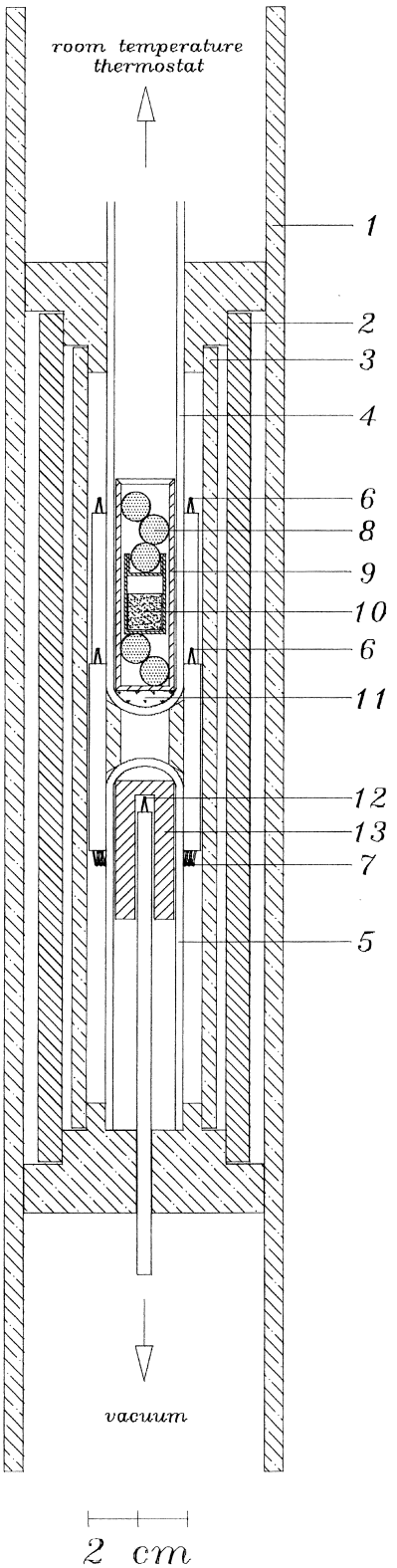

Fig. 4. High temperature drop direct calorimeter [7]. A schematic section of the calorimeter is presented as it appears at the end of a run. It is inserted, inside a furnace, in a (1) vacuum tight work tube, (2) 'nichrome' metallic cylinder, (3) alumina tube, (4, 5) silica tubes forming the measuring and reference cells respectively, (6, 7) sample and reference thermopile junctions, (8) Ag spheres for calibration, (9) sample-receiving metallic vessel, (10) sample enclosed in its metallic crucible, (11) quartz wool, (12) thermocouple, (13) metallic reference block.

furnaces used respectively for electric calibration and for starting the reaction in the sample (about 10–15 g of compacted fine metal powders enclosed in a gas-tight inox crucible sealed by electric welding). The calorimeter, inserted in a large thermostatted Al-block, is covered by the hot junctions of a thermopile (80 Cu/constantan couples) differentially connected to another thermopile placed for reference on a second similar calorimeter.

The energy evaluation, performed in the previous models by means of a standard watt-hour-meter, is now made by using a PC driven acquisition system which measures time and voltage and current of the electric heating coils, and also records the output of the thermopile, control thermocouples, etc.

The heats of formation can be considered to be measured at 300 K. Errors in the range of 2–6% (lower for highly exothermic synthesis) have been estimated.

2.1.2. High-temperature direct synthesis calorimetry

In several cases, the direct synthesis of the alloys can be conveniently carried out in a high-temperature calorimeter. Working at appropriate temperatures, depending on the melting point of alloys and on the rate of the reaction, the enthalpies of formation of low-exothermic compounds may also be obtained. The reaction in a high-temperature calorimeter may be started by dropping into it samples from a lower temperature thermostat (which generally is a room temperature thermostat).

Our high temperature calorimeter is based on this principle; it has been described in [7] and is presented in Fig. 4. It contains two cells set one above the other and located in ceramic and metallic tubes for thermal equalization. The temperature difference between the two cells (working and reference cells) is measured by means of a 20 Pt/PtRh10% couple thermopile.

The sample is a compacted mixture of the powder metals, sealed under argon in a Ta or Mo small container in order to prevent any oxidation and change in the starting composition. The heat effect observed in dropping the sample inside the high temperature calorimetric cell is compared with that observed in dropping the compound. In each run the calibration is made by dropping weighed pieces of pure silver.

The standard deviation for calibration was found to be $\pm 1\%$ at the maximum. The total error of the results is estimated to be in the range of $\pm 3\%$.

3. Results obtained in our laboratory in the thermochemical investigation of some groups of rare earth alloys

3.1. Remarks on previous and current investigations

The rare earth alloy systems which have been studied or are under investigation in our laboratory, are summarized

in the following list, which also includes some indication of the more recent reference literature.

3.1.1. R–Mg

A number of enthalpy of formation data have been reported in literature. These data have been obtained by acid solution calorimetry, vapour pressure and, in the case of Ce alloys, by solution calorimetry in liquid Mg. However, emphasis has been given to the serious discrepancies between the different sets of values and to the need of a revision (see for instance Colinet and Pasturel [8]). A few preliminary measurements on some R–Mg alloys by means of the high temperature calorimeter have been carried out in our laboratory [9].

3.1.2. R–Ni alloys

Several systematic investigations of the R–Ni alloys have been carried out by different researchers (Colinet et al. by Al solution calorimetry [10], Schott and Sommer by Sn solution calorimetry [11], Dischinger and Schaller by e.m.f. [12], Hubbard et al. by acid solution calorimetry [13], Kleppa and co-workers by mixing and drop calorimetry [14] and by high temperature drop calorimetry [2]). A general discussion of the enthalpy of formation of selected R with the elements of this part of the Periodic Table (Ni, Ru, Rh, Pd, Ir, Pt) has been presented by Kleppa (see for instance [2]). While studying some ternary R–Ni–Me systems such as R–Ni–Al alloys [15,16], a few measurements have been started by our group as a reference for selected R–Ni alloys [17].

3.1.3. R–Ag and R–Au alloys

A systematic investigation of this type of alloy (and of those with other 'noble' metals such as Ru, Rh, Pd, Ir, Pt) has been carried out by Kleppa and co-workers. The data relevant to the R–Au alloys (to which some contribution has also been given by our group) will be discussed later (see Section 3.2.). As for the R–Ag alloys, only scarce data are available on thermodynamics. Calorimetric measurements for solid R–Ag alloys (R = Sc, Y, La, Ce) have been reported by Kleppa and co-workers [18,19]. Direct calorimetric investigation on a few R–Ag alloys (on the congruent melting $R_{14}Ag_{51}$ and RAg phases) is now in progress in our laboratory.

3.1.4. R–Zn alloys

Several R–Zn systems have been studied by using vapour pressure measurements [20] and e.m.f. [8]. The minima of the $\Delta_f H$ generally correspond to the RZn_2 compounds. Measurements of the enthalpies of formation of the Nd–Zn alloys have been performed by our group by using direct and HCl solution calorimetry [21]. In spite of the quite different techniques employed and the different temperature ranges involved, a fair agreement with the Chiotti and Mason data [20] was observed.

3.1.5. R–Al alloys

Several R–Al alloys (R = La, Ce, Pr, Nd, Sm and Yb) have been investigated in our laboratory by direct small furnace calorimetry [22]; the high stability of the RAl_2 compounds has been confirmed. A very good agreement with the experimental data by Colinet [23] and Sommer [24] has been observed. These data also fit very well in the trend of the standard enthalpies of formation of aluminides, systematically studied and discussed by Kleppa and coworkers [25].

3.1.6. R–Sn and R–Pb alloys

Several data have been reported in literature mainly for the RSn_3 and RPb_3 phases by e.m.f., vapour pressure measurements, dynamic differential calorimetry and Sn solution calorimetry [8]. For the R–Sn systems, in our laboratory, measurements on Y–Sn, La–Sn and Ce–Sn alloys [26] have been performed by direct small furnace calorimetry and the trends of the enthalpy of formation have been discussed. A re-examination of R–Sn phase diagrams has also been carried out. As for Nd–Sn and Gd–Sn systems, the investigation is in progress [27] by using both small-furnace and high temperature direct calorimetry.

The enthalpies of formation (small-furnace calorimeter) of some R–Pb (R = Y, La, Yb, Lu) alloys have also been measured; the investigation of the Gd–Pb system by direct small furnace calorimetry, is in progress. For these systems, measurements of C_p have also been made. E.m.f. measurements moreover have been considered in addition to the direct calorimetry [28].

3.1.7. R–As systems

Systematic measurements by dynamic differential calorimetry of the heat of formation have been carried out for the NaCl type RAs compounds [29]. For La–As, measurements have also been carried out by direct small furnace calorimetry in our laboratory, as discussed later (see Section 3.2.).

3.1.8. R–Sb and R–Bi alloys

A systematic investigation has been performed in our laboratory on the R–Sb (R = Y, La, Ce, Pr, Nd, Sm, Gd, Er and Dy) [30] and R–Bi (R = Y, La, Ce, Pr, Nd, Sm, Gd, Tb, Dy, Er, Yb) systems [31]: the very high stability of the phases near to the 1:1 composition has been pointed out. The trends of the formation enthalpies have been compared with the shape of the phase diagrams. The data have also been used to optimize the Pr–Sb, Nd–Sb and Sm–Sb phase diagrams and to compute the ternary Nd–Pr–Sb system [32]. The systematic trends of the heats of formation along the trivalent rare earth series have been especially discussed. The particular behaviour of Yb on the other hand has been pointed out [33].

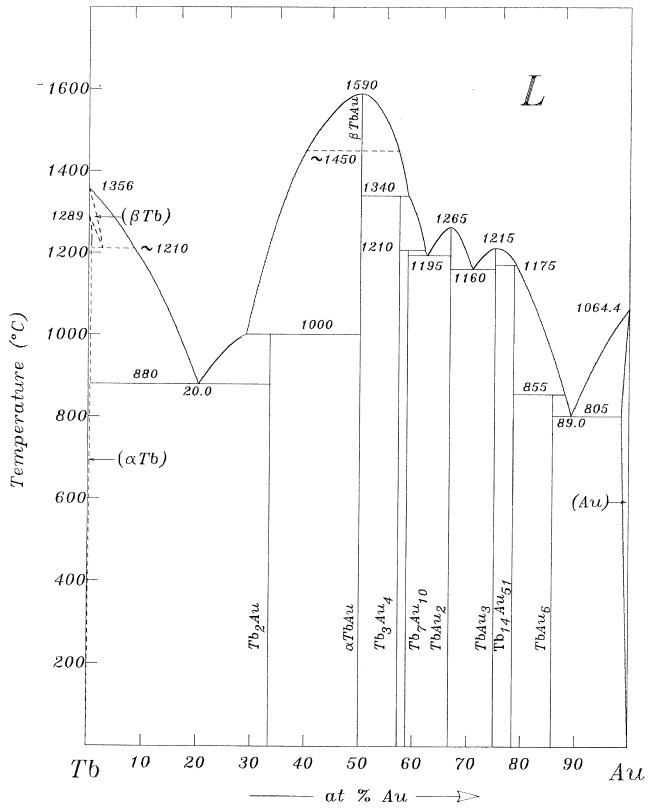

Fig. 5. Phase diagram of the Tb–Au system [36]. The small solid solubility ranges observed especially at high temperature for the TbAu and $Tb_{14}Au_{51}$ are not reported in the figure.

3.1.9. R–Te systems

The results obtained by direct small furnace calorimetry for Ce–Te alloys are presented (see Section 3.2) in this work.

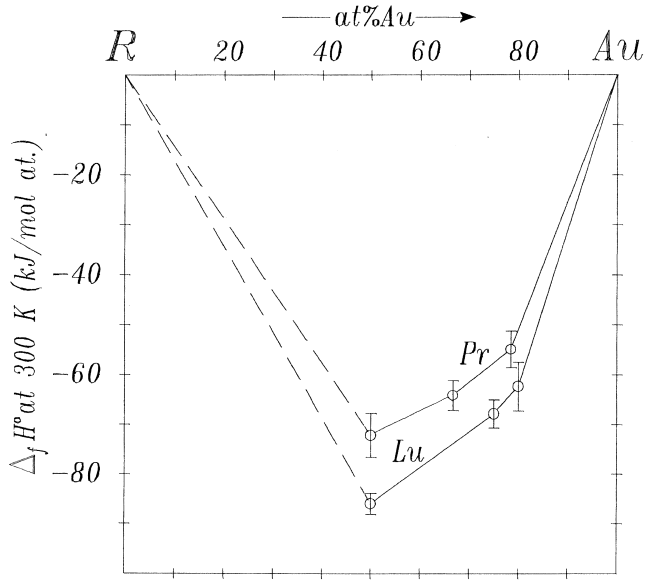

Fig. 6. Standard enthalpies of formation of Pr–Au [39] and Lu–Au [37] solid alloys.

3.2. Results obtained in this work in the study of selected groups of R alloys and compounds

3.2.1. Rare-earth gold alloys

Among the alloys with the ‘noble metals’, a characteristic group of systems is represented by the combinations with Au. These systems are generally characterized by the formation of up to 7–8 phases in each system: R_2Au and RAu are usually present. Moreover, many other phases are formed in the Au-rich composition ranges (typical stoichiometries may be $R_{14}Au_{51}$, RAu_4, RAu_6, etc.). The high stability of several R-Au phases may be related to their high melting points: the Raynor index [34] (which is

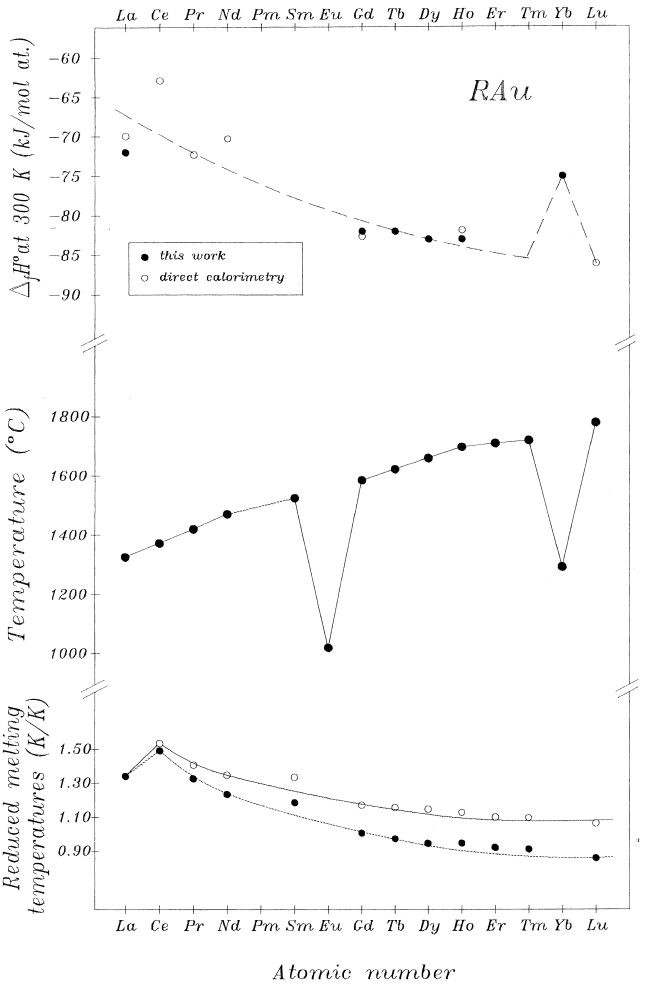

Fig. 7. RAu phases. The trend of melting temperature (°C) and of the corresponding reduced melting temperatures are compared with the trend of the standard enthalpy of formation of solid alloys. The open symbols are data from Kleppa et al. [3,37,39]. In the reduced melting temperature trend, the open symbols correspond to the experimental values of the ratio (K/K) between the melting temperature of the phase and that of the R metal involved. The filled symbols, calculated as the ratio (K/K) between the (constant) melting point of a fixed RAu phase (here LaAu) and the melting point of the different R, define a ‘reference slope’. According to Gschneidner [40], the experimental slope compared with the reference one gives an indication of the stability trend of the phases along the lanthanide series.

Table 1
Heats of formation of solid R–Au alloys. Calorimetric data for the reaction: $(1-x)R_{solid} + xAu_{solid} \rightarrow R_{1-x}Au_{x\ solid}$. Reactions performed in Mo containers, data reduced to 300 K

R	Nominal composition x_{Au}	$-\Delta_f H$ (kJ/mol at.)	Micrographic appearance	Type of Calorimeter and working temperature
La	0.52	71.9[a]	LaAu (primary crystals) surrounded by La_3Au_4 (see Fig. 8).	Small-furnace Room temperature
Ce	0.20	33.7[b]	Ce_2Au dendritic crystals (90%) surrounded by (Ce) solid solution (10%).	Small-furnace Room temperature
Ce	0.30	48.5[b]	Ce_2Au primary crystals (85%) surrounded by (Ce) solid solution (15%).	Small-furnace Room temperature
Gd	0.49	81.4[c]	GdAu primary crystals (95%) plus Gd_3Au_4 (5%).	cal HT $T=1153$ K
Tb	0.49	83.7[d]	TbAu primary crystals (95%) and Tb_3Au_4 (5%) at the grain boundary.	cal HT $T=1147$ K
Tb	0.49	78.4[d]	TbAu primary crystals (90%) and Tb_3Au_4 (10%) at the grain boundary.	cal HT $T=1156$ K
Dy	0.49	81.5[e]	DyAu primary crystals (95%) and incomplete reaction products (5%).	cal HT $T=1171$ K
Dy	0.49	(76.3)	Sample not in equilibrium: DyAu and Dy_3Au_4 crystals (70%) and Au-richest phases (30%).	cal HT $T=1158$ K
Ho	0.49	(75.2[f])	HoAu primary crystals (80%) plus $HoAu_2$ crystals (10%) and other Au-richest phases (10%).	cal HT $T=1171$ K
Yb	0.53	73.6[g]	YbAu primary crystals (80%) plus $YbAu_2$ (20%).	Small-furnace Room temperature
Yb	0.60	72.4[g]	$YbAu_2$ primary crystals (75%) and YbAu (25%).	cal HT $T=1098$ K
Yb	0.65	70.8[g]	$YbAu_2$ primary crystals (85%) surrounded by $YbAu_3$ (15%).	Small-furnace Room temperature

[a] To LaAu the value $\Delta_f H = -72.0 \pm 2.0$ kJ/mol at. has been attributed.
[b] Average $\Delta_f H$ value extrapolated for Ce_2Au: -55.0 ± 1.0 kJ/mol at.
[c] $\Delta_f H$ extrapolated value for GdAu: -82.0 ± 2.0 kJ/mol at.
[d] For TbAu the value $\Delta_f H = -82.0 \pm 2.0$ kJ/mol at. has been interpolated.
[e] To DyAu the value $\Delta_f H = -82.0 \pm 3.0$ kJ/mol at. has been attributed.
[f] For HoAu the value $\Delta_f H = -83.0 \pm 4.0$ kJ/mol at. has been estimated.
[g] For YbAu a value of $\Delta_f H = -75.0 \pm 2.0$ kJ/mol at. has been interpolated.

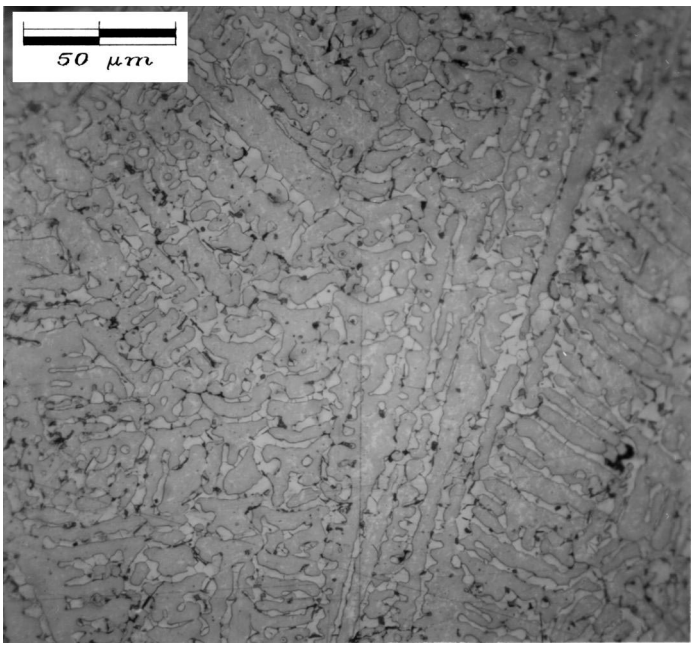

Fig. 8. Optical micrograph of La–52 at% Au. Etched in an alcohol + 1% HNO_3 solution. LaAu (primary crystals) surrounded by La_3Au_4.

defined as $I = T_m(R_{1-x}Au_x)/[(1-x)T_m(R) + xT_m(Au)]$ where T_m are the melting temperatures, in K, of the different substances), reaches values as high as 1.3 for the RAu stoichiometry. This behaviour has been described in detail in [35]. A number of R–Au phase diagrams have been studied in our laboratory (R = Pr, Nd, Gd, Tb and Y). Fig. 5 shows, as an example, the Tb–Au system [36]. As for the formation thermochemistry of these alloys in the solid state, several contributions have been given, mainly by Kleppa and co-workers. Investigations on selected compositions of different R–Au with R = Sc, Y, La, Ce, Pr, Nd [3] and more recently on Gd–Au, Ho–Au and Lu–Au systems [37] have been carried out by high temperature calorimetry.

Some measurements (by using e.m.f. methods) have also been performed for the Y–Au alloys by Alqasmi and Schaller [38].

As an example, Fig. 6 shows, according to Kleppa's work the trends of $\Delta_f H$ vs. composition for Pr–Au [39] and Lu–Au [37] alloys.

For the RAu compounds, the trend of $\Delta_f H$ vs. the atomic number of R is shown in Fig. 7. For these phases, preliminary information about our work has previously been reported [41]. A few more measurements have also been carried out in this work. The results of the different measurements are reported in Table 1. These, together with the information about the completeness of the formation reaction deduced from the metallographic appearance have been used for an evaluation of the formation enthalpies of the compounds reported at the foot of Table 1 and in Fig. 7. An indication of values slightly more exothermic (of 2–3 kJ/mol at.) than those previously indicated [41] has now been reached. We see a general agreement between our data and those from literature.

For the Ce–Au system, for which the literature data show a certain discrepancy from the general average trend, particular difficulties were observed in the preparation of the 1:1 compound. In the Ce-rich region, however, measurements carried out by our small-furnace calorimeter resulted in a reliable enthalpy of formation value extrapolated for Ce_2Au (see Table 1).

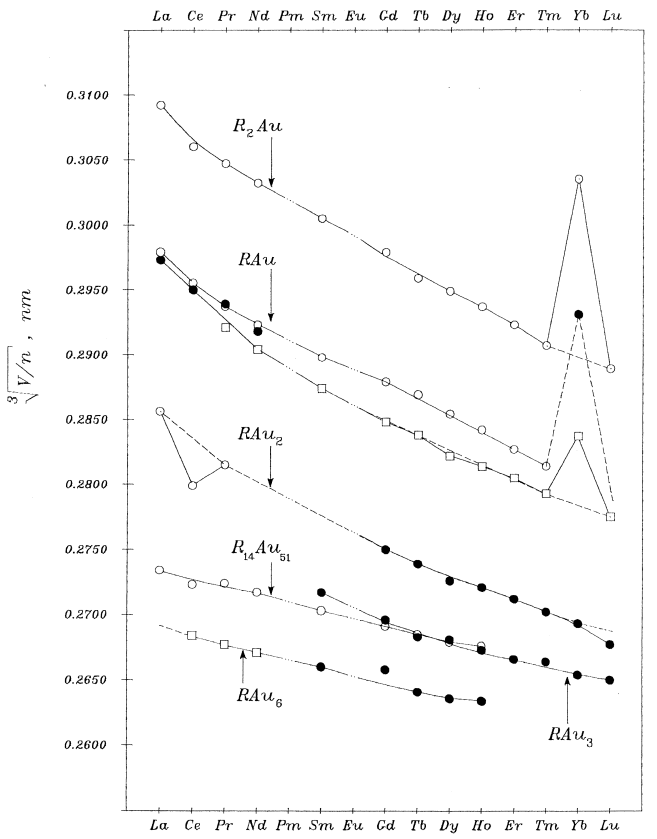

Fig. 9. R–Au phases. Average interatomic distance (obtained as the cube root of the atomic volume) vs. the lanthanide atomic number. R_2Au: (○) *oP12*–Co_2Si type; RAu: (○) *oC8*–CrB type, (●) *oP8*–FeB type and (□) *cP2*–CsCl type; RAu_2: (○) *oI12*–$CeCu_2$ type and (●) *tI6*–$MoSi_2$ type; RAu_3: (●) *oP8*–$TiCu_3$ type; $R_{14}Au_{51}$: (○) *hP65*–$Gd_{14}Ag_{51}$ type; RAu_6: (●) *tP56*–$SmAu_6$ type and (□) *mC28*–$PrAu_6$ type.

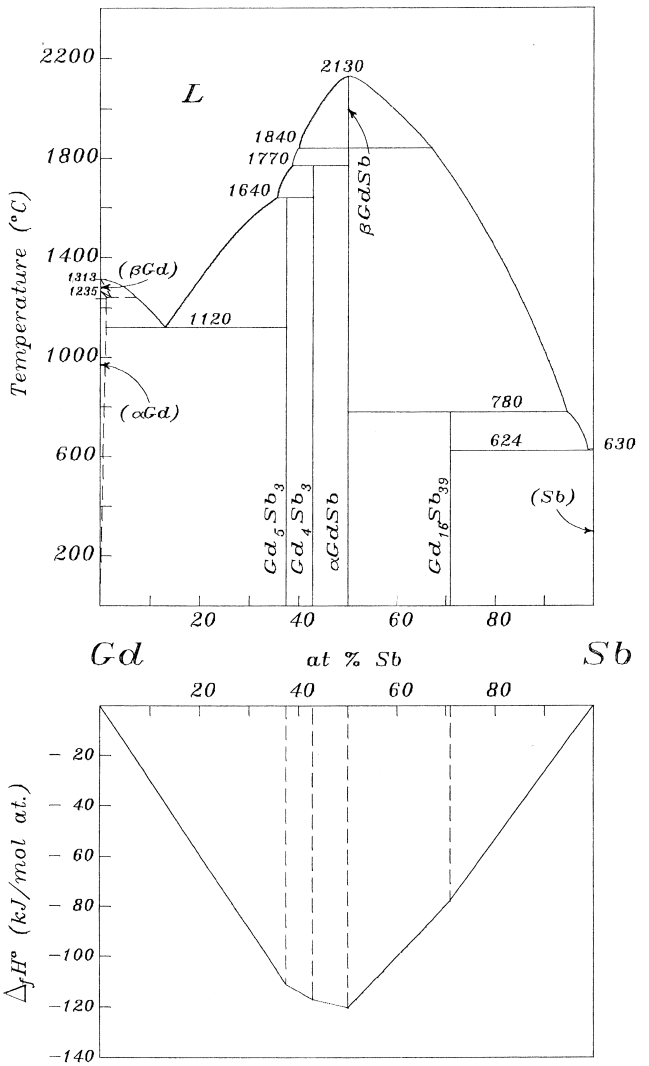

Fig. 10. Gd–Sb system. Trend of the standard formation enthalpy of solid alloys at room temperature compared with the shape of the phase diagram (after [45] with $GdSb_2$ replaced by the recently identified $Gd_{16}Sb_{39}$ [30]).

During this study, the existence moreover of a new Ce_3Au_4 phase was observed and its structure determined: Ce_3Au_4, *hR42*–Pu_3Pd_4 type, $a=1.3887$ nm, $c=0.6170$ nm.

As for YbAu, a slight deviation from the smooth trend of the other R may be noticed in Fig. 7; this may be related to the possible different valence state. As pointed out by Gschneidner [42] in the Yb–Au alloys, a change in the valence state from nearly II for the Yb-rich alloys to about III for the Au-rich alloys has been evidenced. This may also be related to the trend of the averaged interatomic distance reported in Fig. 9 for the R–Au phases. The larger dimensions of Yb(II) in the Yb-richer compounds is evident from the deviation from the trend of the trivalent rare earths. It has frequently been observed in literature that thermochemical data may also be related to the valence state [33,42–44]. When no promotion energy term (from one valence state to another) is involved, i.e. the metal valence value (II for Eu and Yb, mainly III for the others) is the same in the alloy as in the metal, all the data relevant to all the R lie on a regular monotonic line. The small deviation from the trivalent values shown by Yb in the YbAu compound may agree with an intermediate (partially divalent) value of the valence. Fig. 7 shows moreover the good correlation between the $\Delta_f H$ trend and those of other constitutional properties (melting points).

3.2.2. R–X alloys (X=As, Sb, Bi, Te)

As previously mentioned, another family of alloys (also strongly exothermic) which have been extensively studied (and are still under investigation) in our laboratory are those given by the elements of the 15th and 16th groups of the Periodic Table.

Among the compounds with the elements of the 15th group, we have made a particular study of the antimonides, bismuthides and several arsenides. Some of the characteristic features of these systems are represented, as an example, in Fig. 10 in which the data recently obtained for the Gd–Sb system [30] are reported. We notice the high values of the melting points and the nearly symmetric

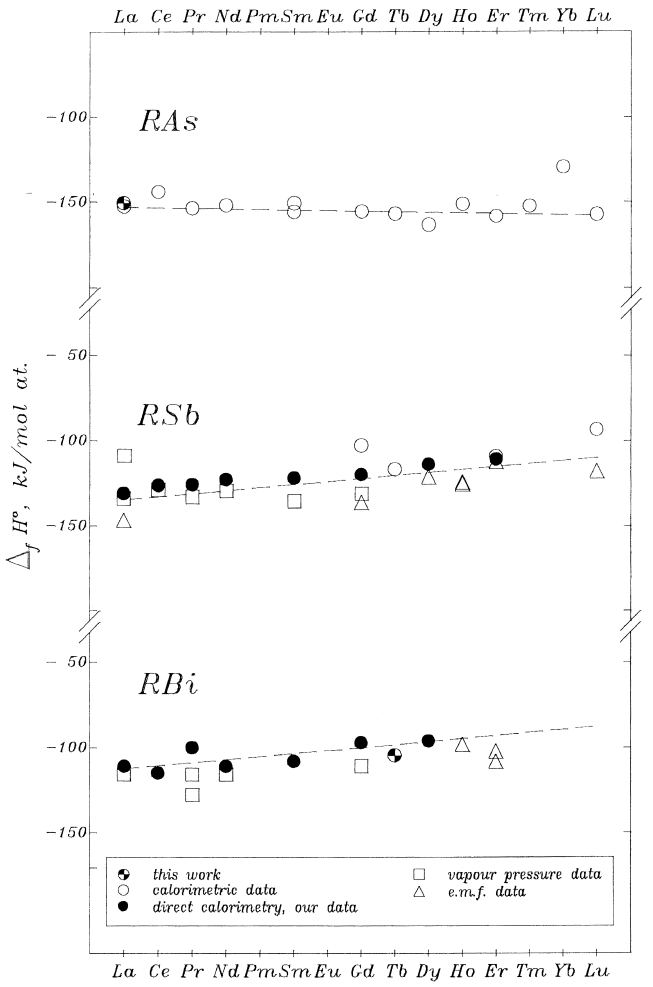

Fig. 11. Standard enthalpy of formation at room temperature of RX compounds (X=As, Sb, Bi) vs. the lanthanide atomic number. For RSb, a selection of the calorimetric data reported by [46] has been done.

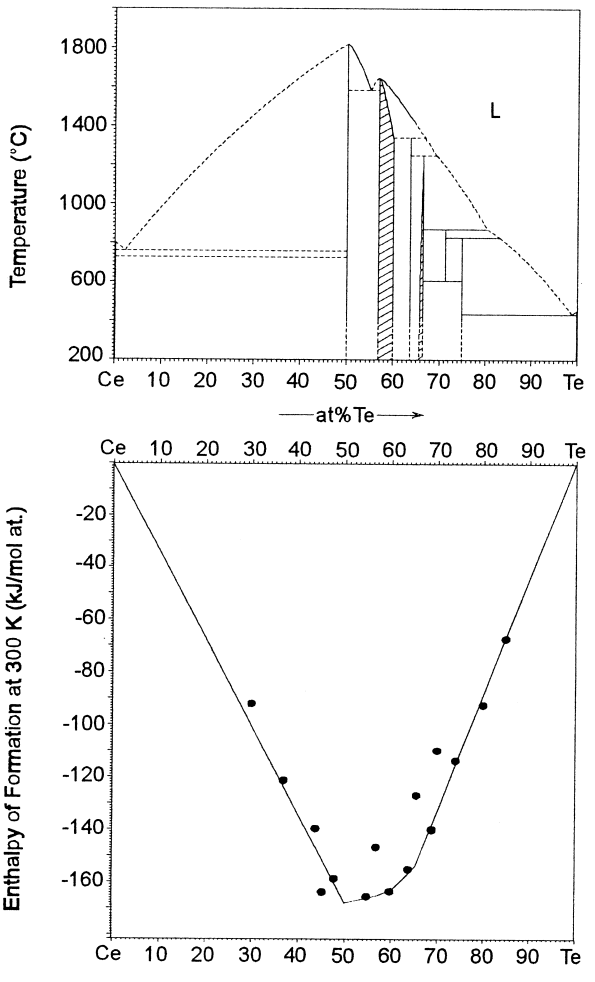

Fig. 12. Ce–Te system. Tentative phase diagram [1] and data of the standard enthalpy of formation of solid alloys at 300 K obtained by using small-furnace direct calorimetry: (●) experimental values; (—) interpolated trend.

shape of the liquidus curve around the 1:1 composition. A good correlation may be observed with the $\Delta_f H$ of the solid alloys, with a deep minimum for the same composition. Similar behaviour is presented by the various R–Sb, R–Bi and also R–As systems. Several groups of isostructural compounds are moreover characteristic of these systems: we may mention the RX compounds given by nearly all the R (with some exception for the divalent ones) having the *cF8*–NaCl type structure, and the R_4X_3 phase (*cI28*–anti-Th_3P_4 type). For the different RX compounds (X = As, Sb, Bi) the values known from literature for the ΔH of formation are reported in Fig. 11 together with those obtained in this work for TbBi ($\Delta_f H = -104.0 \pm 2.0$ kJ/mol at. by high temperature direct calorimetry) and LaAs ($\Delta_f H = -150.0 \pm 3.0$ kJ/mol at. by room temperature small-furnace isoperibol calorimetry, see also [47]). For RAs, the good agreement with the value obtained by Hanks and Faktor [29] (−153 kJ/mol at.) may be considered.

For the monoantimonides and monobismuthides, the general good agreement of our data with those reported in literature may be noticed (see Fig. 11), even if there seems to be a slight systematic difference between the vapour pressure (and e.m.f.) data and the calorimetric ones, which on average, seem to be slightly less exothermic. An indication of decreasing values of the negative enthalpy of formation along the lanthanide series may be noticed.

As for the compounds of the 16th group, these are (especially for oxygen and sulfur) much more ionic and covalent in their bonding mechanism. Much higher values of the (negative) ΔH of formation have been reported in literature especially on passing from the heavy to the light (sulfur, oxygen) elements of this group. For the oxides and sulfides several data are reported in literature. Gschneidner [48], for instance, reported as a function of temperature the ΔG of formation of the more stable R oxides and sulfides. These values have been discussed in comparison with those relevant to the other metals, and the high stability of the R compounds underlined.

As a general comment to the R–X systems (with X = S, Se, Te) we may note the high complexity (high number of compounds, transformations, etc.) of the diagrams (especially for the compositions corresponding to at% X > 50). For most of these systems a clear definition of the equilibria is lacking. In fact, the high melting temperatures, the sequence of numerous intermediate phases (both point and solid solution phases) showing complex formation (and decomposition) equilibria, often resulted in uncertain state diagrams which, in several cases, show improbable trends of the equilibrium lines. In fact, contradictory assessment of the same data have been reported in some cases [49].

Our laboratory is attempting to make some contribution to the knowledge of the thermochemistry of these systems by performing some calorimetric work on the less exothermic compounds of the group, namely on the tellurides. However, difficulties have been encountered: the R–X direct reaction synthesis may in fact result in sudden, explosive, evolution of heat, not always giving samples in an equilibrium state.

Table 2
Heats of formation of solid Ce–Te alloys. Calorimetric data for the reaction[a]: $(1-x)Ce(\gamma)_{solid} + xTe_{solid} \rightarrow Ce_{1-x}Te_{x\ solid}$ at 300 K

Nominal composition x_{Te}	$-\Delta H$ (kJ/mol at.)	Diffraction lines observed in the powder diffraction photograph and remarks
0.30	91.7	CeTe + Ce
0.375	122.4	CeTe + Ce
0.43	140.8	CeTe
0.45	164.7	CeTe
0.48	159.5	CeTe
0.55	166.4	CeTe + Ce_3Te_4 + *x*
0.58	(147.2)	Sample not in equilibrium
0.60	163.5	Ce_3Te_4
0.65	155.3	Mainly $CeTe_2$
0.675	(129.0)	Sample not in equilibrium
0.70	139.3	$CeTe_2$ + *x*
0.70	(110.0)	Sample not in equilibrium
0.75	113.5	$CeTe_3$ + *x*
0.80	92.6	$CeTe_3$ + *x*
0.85	67.8	$CeTe_3$ + *x*

[a] Values interpolated for CeTe: −168 ± 4 kJ/mol at. for Ce_3Te_4–Ce_2Te_3: −163 ± 4 kJ/mol at.

For the Ce–Te system (for which a provisional diagram is reported in Fig. 12) a number of samples have been prepared in the room temperature, small-furnace aneroid isoperibol calorimeter. Of the different alloys prepared (about 40), only a dozen resulted in equilibrium, these samples have been considered to give reliable data. A selection of the data obtained is reported in Table 2 and in Fig. 12. In spite of the experimental difficulties and of the large fraction of unusable samples, we believe that the overall trend of $\Delta_f H$ plotted in Fig. 12 (and the interpolated values reported in Table 2) and possibly the indication of the minimum may be considered significant.

This, in a way, may be confirmed by Fig. 13 where the data relevant to a few RTe_x compounds found in literature have been reported. No trend of course may be deduced, notice however the fair agreement among the numerical order of the different values.

4. Final remarks

With reference also to the comments reported in the introduction, we may compare the data just reported for the Ce–Te system to those relevant to the R–X systems for X selected in the groups 15, 14, 13 and 12. We see in Fig. 14 the progressive change in the value and position of the minima of the curves of $\Delta_f H$ vs. composition.

As a conclusion, we may consider the summary of the experimental data reported in Fig. 1 and here compared (see Fig. 15) with those computed for La–Me according to

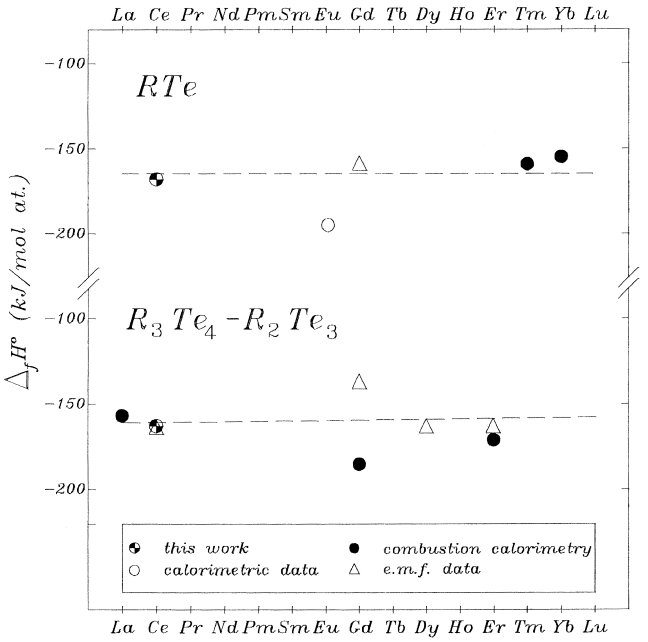

Fig. 13. Literature data of the enthalpies of formation of solid RTe and R_3Te_4–R_2Te_3 compounds. The calorimetric data were mainly obtained by drop calorimetry [50], combustion calorimetry [51,52] and fluorine combustion calorimetry [53]; e.m.f. data are mainly from [54–59].

the Miedema model [63,64]. We notice the overall agreement between the two schemes and the corresponding subdivision of the elements into two families forming or non-forming compounds, reacting with negative or zero or positive $\Delta_f H$ which well reproduce the binary combination characteristics reported and discussed above.

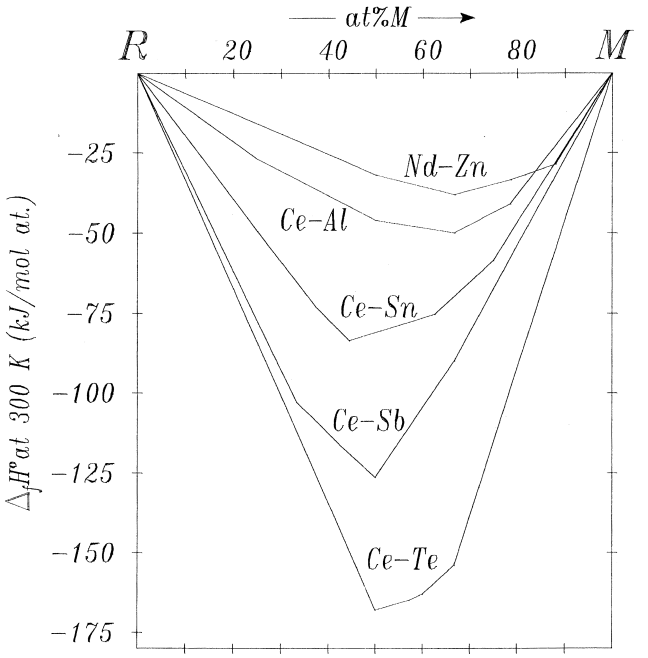

Fig. 14. Enthalpies of formation of Nd–Zn [21], Ce–Al [60], Ce–Sn [61], Ce–Sb [62], Ce–Te (this work) solid alloys at 300 K.

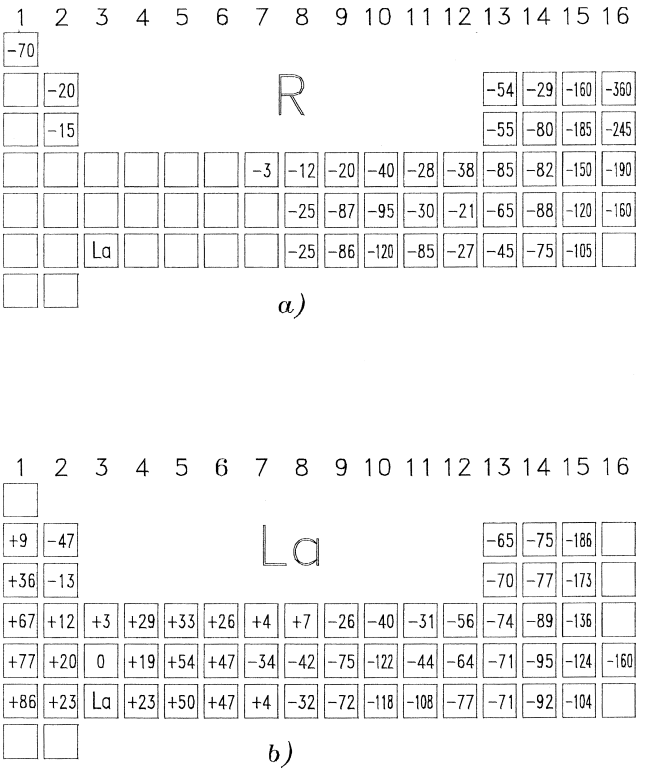

Fig. 15. Enthalpy of formation relevant to the different R–Me systems (for a summary of the thermochemical behaviour, compare also with Fig. 1). Comparison between experimental and calculated data: (a) minimum experimental values (averaged over the different trivalent R) observed in each system. (b) Minimum values computed for each La–Me system according to [63]. The computed value for La–Te is from [64].

Acknowledgements

The planning and development of the studies here presented form a part of an Italian National Research Project entitled: ‘Leghe e composti intermetallici: stabilità termodinamica, proprietà fisiche e reattività’. The authors would like to thank the Italian Ministero della Ricerca Scientifica e Tecnologica (Programmi di Ricerca Scientifica di Rilevante Interesse Nazionale) for the financial support afforded them. Partial financial support was obtained also in the framework of the Italian ‘Progetto Finalizzato Materiali Speciali per Tecnologie Avanzate II’.

This paper corresponds to an invited lecture presented at the ‘Kleppa Symposium on High Temperature Termochemistry of Materials’ (129th TMS Annual Meeting and Exhibition – March 2000, Nashville). The authors express to Dr. Prof. Kleppa their compliments and best wishes.

References

[1] T.B. Massalski, H. Okamoto, P.R. Subramanyan, L. Kacprzak (Eds.), 2nd Edition, Binary Alloy Phase Diagrams, Vols. 1–3, Metals Park, OH, 1990.

[2] Q. Guo, O.J. Kleppa, Z. Metallkd. 87 (1996) 10.
[3] O.J. Kleppa, J. Phase Equilibria 15 (1994) 240.
[4] O. Kubaschewski, W.A. Dench, Acta Metall. 3 (1955) 339.
[5] R. Capelli, R. Ferro, A. Borsese, Thermochim. Acta 10 (1974) 13.
[6] R. Ferro, G. Borzone, N. Parodi, G. Cacciamani, J. Phase Equilibria 15 (1994) 317.
[7] G. Cacciamani, G. Borzone, R. Ferro, J. Alloys Comp. 220 (1995) 106.
[8] C. Colinet, A. Pasturel, in: K.A. Gschneidner Jr., L. Eyring (Eds.), Handbook on the Physics and Chemistry of Rare Earths, Vol. 19, North-Holland, Amsterdam, 1994, p. 479.
[9] G. Cacciamani, G. Borzone, R. Ferro, in: Proc. Thermodynamics of Alloys Meeting, Marseille, 1996, p. 65.
[10] C. Colinet, A. Pasturel, A. Percheron-Guegan, J.C. Achard, J. Less-Common Met. 134 (1987) 109.
[11] J. Schott, F. Sommer, J. Less-Common Met. 119 (1986) 307.
[12] J. Dischinger, H.-J. Schaller, Ber. Bunsenges. Phys. Chem. 9 (1998) 1167.
[13] W.N. Hubbard, P.L. Rawlins, P.A. Connick, R.E. Stedwell, P.A.G. O'Hare, J. Chem. Thermodyn. 15 (1983) 785.
[14] S. Watanabe, O.J. Kleppa, Chem Thermodyn. 15 (1983) 633.
[15] G. Borzone, N. Parodi, R. Ferro, in: Y.A. Chang, F. Sommer (Eds.), Thermodynamics of Alloy Formation, TMS, Warrendale, Pennsylvania, 1997, p. 59.
[16] R. Raggio, G. Borzone, R. Ferro, in: Proc. XXth AICAT-GICAT National Congress 'Calorimetry, Thermal Analysis, Experimental Thermodynamics', Roma (Italy), December 14–18, 1998, pp. C–SC 8.
[17] G. Borzone, N. Parodi, R. Raggio, R. Ferro, in: Proc. 13th International Conference on Solid Compounds of Transition Elements, Stresa (Italy) 4–7 April, 2000, p. PA14.
[18] K. Fitzner, W.G. Jung, O.J. Kleppa, Metall. Trans. 22A (1991) 1103.
[19] K. Fitzner, O.J. Kleppa, Metall. Trans. 24A (1994) 1827.
[20] P. Chiotti, J.T. Mason, Metall. Trans. 4 (1973) 1527.
[21] G. Borzone, G. Cacciamani, R. Ferro, J. Charles, J. Hertz, J. Less-Common Met. 128 (1987) 297.
[22] G. Borzone, A.M. Cardinale, N. Parodi, G. Cacciamani, J. Alloys Comp. 247 (1997) 141.
[23] C. Colinet, A. Pasturel, K.H.J. Buschow, J. Chem. Thermodynamics 17 (1985) 1133.
[24] F. Sommer, M. Keita, H.G. Krull, B. Predel, J. Less-Common Met. 137 (1988) 267.
[25] W.-G. Jung, O.J. Kleppa, L. Topor, J. Alloys Comp. 176 (1991) 309.
[26] G. Borzone, A. Borsese, R. Ferro, Z. Anorg. Allg. Chem. 501 (1983) 199.
[27] S. Besana, E. Hayer, G. Borzone, in: Proc. Journées d'Etude des Equilibres entre Phases, 23–24 Mars, Marseille (France), 2000, p. 93.
[28] G. Borzone, N. Parodi, R. Ferro, M. Gambino, V. Vassiliev, J.P. Bros, J. Alloys Comp. 220 (1995) 111.
[29] R. Hanks, M.M. Faktor, Trans. Faraday Soc. 63 (1967) 1130.
[30] G. Borzone, M.L. Fornasini, N. Parodi, R. Ferro, Intermetallics 8 (2000) 189.
[31] G. Borzone, N. Parodi, R. Ferro, J. Phase Equil. 14 (1993) 485.
[32] G. Cacciamani, R. Ferro, H.L. Lukas, Z. Metallkd. 83 (1992) 9.
[33] G. Borzone, R. Ferro, N. Parodi, A. Saccone, Gazz. Chimica Italiana 125 (1995) 263.
[34] G.V. Raynor, J. Less-Common Met. 29 (1972) 333.
[35] A. Saccone, D. Macciò, S. Delfino, R. Ferro, Metall. Mater. Trans. A 30A (1999) 1169.
[36] A. Saccone, D. Macciò, S. Delfino, R. Ferro, Intermetallics 8 (2000) 229.
[37] K. Fitzner, O.J. Kleppa, Metall. Mater. Trans. 28A (1997) 187.
[38] R.A. Alqasmi, H.-J. Schaller, Z. Metallkd. 84 (1993) 9.
[39] K. Fitzner, O.J. Kleppa, Metall. Mater. Trans. 25A (1994) 1495.
[40] K.A. Gschneidner Jr., J. Less-Common Met. 17 (1969) 1.
[41] G. Borzone, R. Raggio, R. Ferro, Phys. Chem. Chem. Phys. 1 (1999) 1487.
[42] K.A. Gschneidner Jr., F.W. Calderwood, in: T.B. Massalski, W.B. Pearson, L.H. Bennet, Y.A. Chang (Eds.), Noble Metal Alloys, The Metallurgical Society, Inc., Warrendale, PA, 1986, p. 335.
[43] K.A. Gschneidner Jr., J. Less-Common Met. 17 (1969) 13.
[44] K.A. Gschneidner Jr., Met. Mater. Proc. 1 (1990) 241.
[45] M.N. Abdusalyamova, O.R. Burnashev, K.Y. Mironov, J. Less-Common Met. 125 (1986) 1.
[46] K.S. Chua, J.N. Pratt, Thermochim. Acta 8 (1974) 409.
[47] G. Borzone, A. Borsese, R. Ferro, Gazz. Chimica Italiana 113 (1983) 235.
[48] K.A. Gschneidner Jr., B.J. Beaudry, J. Capellen, in: Properties and Selection: Nonferrous Alloys and Special-Purpose Materials, Vol. 2, ASM International, Metals Park, OH, 1990, p. 720.
[49] K.A. Gschneidner Jr., J. Phase Equilibria 13 (1992) 586.
[50] O.D. McMasters, K.A. Gschneidner Jr., E. Kaldis, G. Sampietro, J. Chem. Thermodynamics 6 (1974) 845.
[51] K.A. Sharifov, Z.Sh. Karaev, T.Kh. Azizov, Izv. Akad. Nauk. SSSR, Neorg. Mater. 3 (1967) 719.
[52] A.P. Agaev, K.A. Sharifov, Uch. Zap. Azerb. Univ., Ser. Khim. Nauk. 3 (1972) 72.
[53] H. Spychiger, E. Kaldis, B. Fritzler, Revue de Chimie Minérale 23 (1986) 634.
[54] A.S. Abbasov, T.K. Azizov, A.G. Guseinov, A.B. Agaev, Izv. Akad. Nauk. SSSR, Neorg. Mater. 7 (1987) 1217.
[55] T.K. Azizov, A.S. Abbasov, F.M. Mustafaev, I.Y. Aliev, Vses Konf Kalorim. [Rasshir. Tezisy Dokl.], 7th, 1 (1977) 30.
[56] T.K. Azizov, A.B. Agayev, A.S. Abbasov, A.G. Guseinov, Dokl. Akad. Nauk Az. SSR 36 (1980) 37.
[57] A.G. Guseinov, A.S. Abbasov, A.A. Kuliev, T.K. Azizov, Dokl. Akad. Nauk Az. SSR 40 (1984) 31.
[58] A.P. Somov, A.V. Nikolskaya, Y.I. Gerasimov, Izv. Akad. Nauk. SSSR, Neorg. Mater. 9 (1973) 575.
[59] V.P. Vasiliev, V.I. Goryacheva, Ya.I. Gerasimov, T.S. Lazareva, Vestnik Moskovkogo Universiteta. Khimiya, 35 (1980) 339; Engl. Transl., Moscow Univ. Chem. Bull. 35 (1980) 36.
[60] G. Borzone, G. Cacciamani, R. Ferro, Metall. Trans. 22A (1991) 2119.
[61] G. Borzone, A. Borsese, R. Ferro, J. Less-Common Met. 85 (1982) 195.
[62] A. Borsese, G. Borzone, D. Mazzone, R. Ferro, J. Less-Common Met. 79 (1981) 57.
[63] F.R. deBoer, R. Boom, W.C. Mattens, A.R. Miedema, A.K. Niessen, in: F.R. de Boer, D.G. Pettifor (Eds.), Cohesion in Metals. Transition Metal Alloys, North-Holland, Amsterdam, 1989.
[64] B. Eichler, H. Rossbach, H. Gäggeler, J. Less-Common Met. 163 (1990) 297.